



Molecular Structure, Frontier Molecular Orbitals, MESP and UV–Visible Spectroscopy Studies of Ethyl 4-(3,4-dimethoxyphenyl)-6-methyl-2-oxo-1,2,3,4-tetrahydropyrimidine-5-carboxylate: A Theoretical and Experimental Appraisal

**VISHNU ASHOK ADOLE¹, BAPU SONU JAGDALE^{1*},
THANSING BHAVSING PAWAR,² and BHATU SHIVAJI DESALE¹**

¹Department of chemistry, Arts, Science and Commerce College, Manmad, Taluka-Nandgaon, District- Nashik, India-423104. (Affiliated to Savitribai Phule Pune University, Pune (MH), India).

²Research Centre in Chemistry, Loknete Vyankatrao Hiray Arts, Science and Commerce College Panchavati, Nashik-422003, India (Affiliated to Savitribai Phule Pune University, Pune (MH), India).

Abstract

In the current investigation, we wish to report a combined study on the theoretical and experimental investigation of structural, molecular, and spectral properties of ethyl 4-(3,4-dimethoxyphenyl)-6-methyl-2-oxo-1,2,3,4-tetrahydropyrimidine-5-carboxylate (EDMT). The EDTM molecule is synthesized and characterized by UV-Visible, FT-IR, ¹H NMR, ¹³C NMR, DEPT, and mass spectral techniques. The density functional theory (DFT) investigation was performed by using the B3LYP level of theory at 6-311++G (d,p) basis set. Frontier molecular orbital (FMO) analysis is likewise examined. An TD-DFT method was used for the UV-Visible spectral analysis by using the B3LYP level and 6-311++G (d,p) basis set in the DMSO solvent. Experimental and theoretical UV-Visible spectra were compared in the present study. Various reactivity descriptors are discussed. Besides, Mulliken atomic charges, molecular electrostatic surface potential (MESP), and some valuable thermodynamic functions are studied.



Article History

Received: 09 Jun 2020
Accepted: 24 July 2020

Keywords:

DFT;
TD-DFT;
Ethyl
4-(3,4-dimethoxyphenyl)-
6-methyl-2-oxo-
1,2,3,4-tetrahydropyrimidine-5-
Carboxylate;
6-311++G (d,p);
UV-Visible.

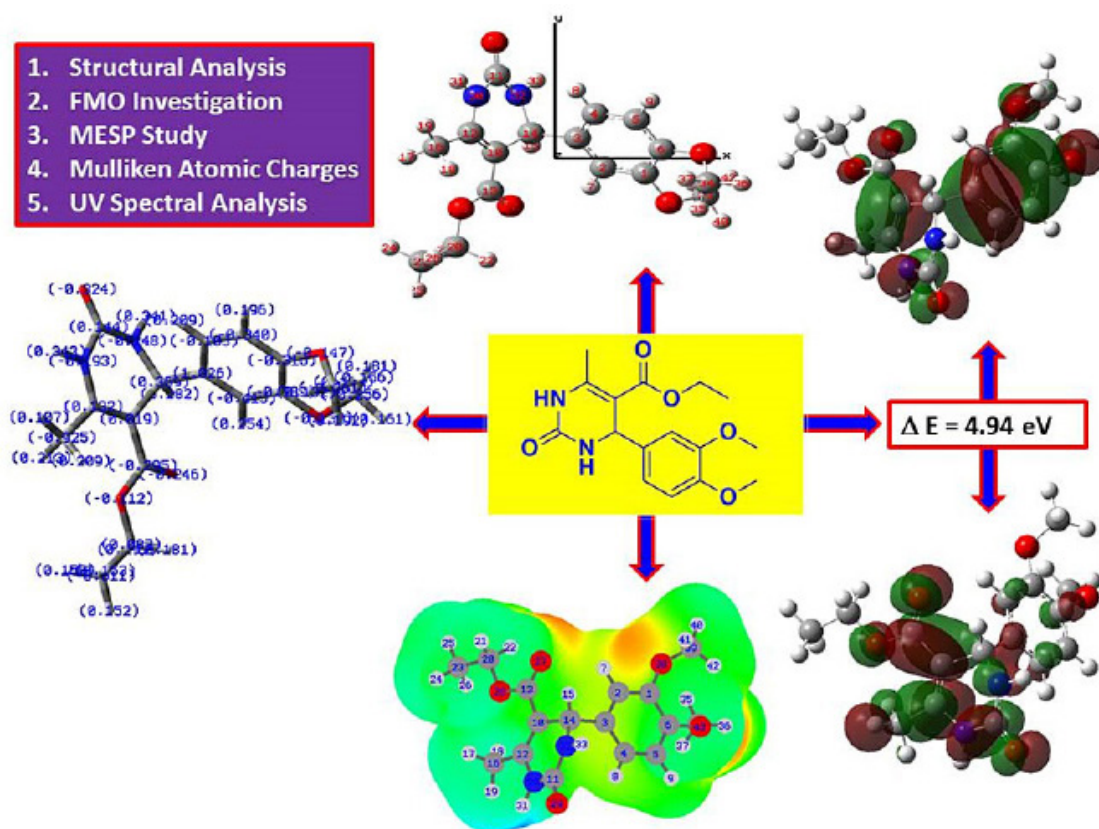
CONTACT Bapu Sonu Jagdale ✉ jagdalebs@gmail.com 📍 Department of chemistry, Arts, Science and Commerce College, Manmad, Taluka-Nandgaon, District- Nashik, India-423104. (Affiliated to Savitribai Phule Pune University, Pune (MH), India).



© 2020 The Author(s). Published by Oriental Scientific Publishing Company

This is an Open Access article licensed under a Creative Commons Attribution-NonCommercial-ShareAlike 4.0 International License
Doi: <http://dx.doi.org/10.13005/msri.17.special-issue1.04>

Graphical abstract



Introduction

3,4-dihydropyrimidin-2(1H)-ones (DHPMs) have developed as useful building blocks for designing new compounds with an expansive assortment of biological applications.¹⁻³ They have gotten a lot of consideration because of the intriguing pharmacological properties related to this heterocyclic framework. DHPMs have been found to display an expansive scope of biological activities such as antitumor,⁴ antitubercular,⁵ antimalarial,⁶ antiviral,⁷ analgesic,⁸ antibacterial,⁹ anti-inflammatory,¹⁰ antifungal,^{10,11} antidiabetic,¹² antiproliferative activities,¹³ etc. Besides, they have additionally been seen as dynamic calcium channel blockers and antihypertensive specialists.^{14,15} To the extent that the materials science is concerned, the DHPMs have been adequately used to develop heterocyclic compounds with fine optical properties. In materials science, DHPMs are progressively discovering applications in the advancement of materials. To a great extent examined applications

in material science are the advancement in functional polymers, adhesives, and fabric dyes.¹⁶⁻¹⁸ Eco-friendly approaches are widely accepted and have been used to reduce environmental hazard.¹⁹⁻²⁸ Many green environment-friendly methodologies were researched for creating newer DHPMs as the biological core. The most common synthetic pathways to DHPMs are microwave irradiation, ultrasound irradiation, ionic liquid strategies, nanoparticles as heterogeneous catalysts, grinding, and solvent-free methods.²⁹ DFT computations are reliable and noteworthy for deciding the structural, electronic, and spectral properties of the molecules.³⁰⁻⁴⁴ Theoretical quantum computations derived from the DFT strategy have been productively utilized in different fields. The examination of spectroscopic and quantum chemical parameters is by all accounts essential to investigate the chemical behavior of the molecules. Considering all these discussed talked about imperative parts, in this, we wish to report theoretical and experimental studies on molecular

structure, HOMO-LUMO analysis, MESP study, and UV-Visible spectral investigation of ethyl 4-(3,4-dimethoxyphenyl)-6-methyl-2-oxo-1,2,3,4-tetrahydropyrimidine-5-carboxylate. In the current research, DFT examination on molecular structure, bond length, bond angle, Mulliken atomic charges have been discussed. The important parameters such as total energy, HOMO-LUMO energies, charge distribution, thermodynamic properties, etc. also studied using the DFT method. Importantly experimental and theoretical comparison on UV-Visible spectra has been discussed.

Methodology

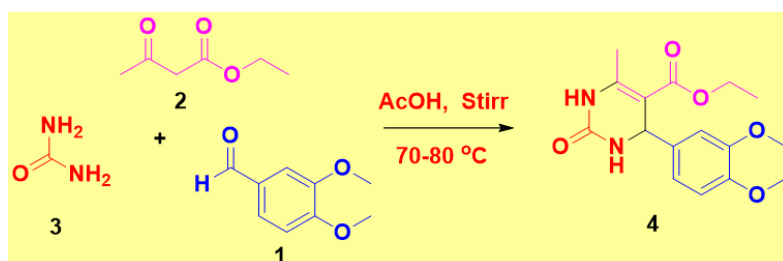
General Remarks

The chemicals with high purity were bought from Local distributor, Nashik. The chemicals were utilized as gotten with no further refinement. NMR spectra were recorded on a sophisticated multinuclear FT

NMR Spectrometer model Advance-II (Bruker) with ^1H frequency 400 MHz and ^{13}C frequency 100 MHz using DMSO- d_6 as a solvent. FT-IR spectra were acquired with potassium bromide pellets on SHIMADZU spectrometer. Aluminium sheets with silica gel 60 F254 (Merck) were used to monitor the reaction.

Experimental Procedure for the Synthesis EDMT

A mixture of 3,4-dimethoxy benzaldehyde (0.01 mol), urea (0.01 mol), and ethyl acetoacetate, (0.01 mol) were mixed in 10 mL acetic acid taken in a conical flask. The resulting mixture was stirred on a magnetic stirrer at 70-80°C until the formation of the desired product (checked by TLC). The crude product was transferred into a beaker containing crushed ice, stirred, filtered, dried naturally, and recrystallized to furnished pure white solid (m.p. 178°C -180°C) (Scheme 1).



Scheme 1 Synthesis of EDMT

Computational Details

All the calculations were performed utilizing DFT strategy with B3LYP/6-311++G (d,p) basis sets in the Gaussian 03 W program.⁴⁵ The geometry of the title compound was optimized and the corresponding energy was determined with a 6-311++G (d,p) basis set. Accordingly, the optimized geometrical parameters, energy, atomic charges, dipole moment, and other thermodynamic parameters were calculated theoretically. Also, the theoretical UV-Visible spectrum of the title compound is correlated with the experimental UV-Visible spectrum. Gauss View 4.1 molecular visualization program has been considered to get visual animation. The electronic properties, for example, HOMO-LUMO energies, absorption wavelengths, and oscillator strengths were computed using the B3LYP method of the TD-DFT) and 6-311++G (d,p) basis set.

Results and Discussion

Spectral Analysis

The detailed spectral results are tabulated in Table 1. The UV-Visible spectrum (Figure 1) indicates that the compound EDMT has λ_{max} value 278 nm which corresponds to electronic excitation from HOMO-LUMO transitions. The FT-IR spectrum (Figure 2) confirms various types of stretching and bending vibrations. The vibrational bands at 3248.13 and 3093.82 cm^{-1} are due to the two N-H groups' stretching vibrations. The vibrational band at 2962.66 cm^{-1} is due to sp^3 C-H stretching vibrations. The 1627.92 cm^{-1} absorption signal is because of the carbonyl group flanked between two N-H groups. Other signals are also in acceptable concurrence with the structure of the EDMT molecule. The ^1H NMR spectrum (Figure 3) finds the types and the total count of the hydrogen atoms in the molecule.

There are total of ten types of protons in the title molecule and therefore has furnished ten signals in the ^1H NMR spectrum. The two NH group signals are 9.16 (s, 1H) and 7.69 (s, 1H). All other signals are correctly matched with the structure of the EDTM molecule. The ^{13}C NMR spectrum (Figure 4) predicts types of carbons atoms in the molecule and therefore one can anticipate the skeleton of the molecule. There are total of sixteen types of carbons that have displayed sixteen signals in the ^{13}C NMR spectrum

affirming the structure. The two signals 165.94 and 152.77 δ are due to carbonyl carbons of ester and amide groups respectively. From the DEPT spectrum (Figure 5), protonated carbons are differentiated from quaternary carbons. There are eight up signals and one down signal in the DEPT spectrum. Out of the eight up signals, four are methyl and on four are methyne groups. The Mass spectrum (Figure 6) has a molecular ion peak at $m/z = 320$ and a base peak at $m/z = 291$.

Table 1: Spectral results of title compound

Type of spectra	Spectral results
UV-Visible (Solvent = DMSO, nm)	278.00
FT-IR (KBr, cm^{-1})	3248.13, 3093.82, 2962.66, 1627.92, 1442.75, 1226.73, 1149.57, 763.81
^1H NMR (400 MHz, DMSO- d_6 , δ)	1.11 (t, $J = 7.0$ Hz, 3H), 2.24 (s, 3H), 3.71 (s, 6H), 3.99 (q, $J = 7.0$ Hz, 2H), 5.09 (d, $J = 3.8$ Hz, 1H), 6.72 (dd, $J = 8.2, 2.1$ Hz, 1H), 6.84 (d, $J = 2.1$ Hz, 1H), 6.89 (d, $J = 8.2$ Hz, 1H), 7.69 (s, 1H), 9.16 (s, 1H)
^{13}C NMR (100 MHz, DMSO- d_6 , δ)	14.68, 18.28, 53.96, 55.90, 56.02, 59.70, 99.86, 110.91, 112.21, 118.38, 137.84, 148.53, 148.68, 148.95, 152.77, 165.94
DEPT (100 MHz, DMSO- d_6 , δ)	14.68 (CH ₃), 18.28 (CH ₃), 53.97 (CH), 55.90 (OCH ₃), 56.02 (OCH ₃), 110.90 (Ar CH), 112.20 (Ar CH), 118.38 (Ar CH) (all up), 59.70 (OCH ₂) (down)
MASS (m/z)	320 (M ⁺), 291, 273, 247, 183, 156, 137, 110

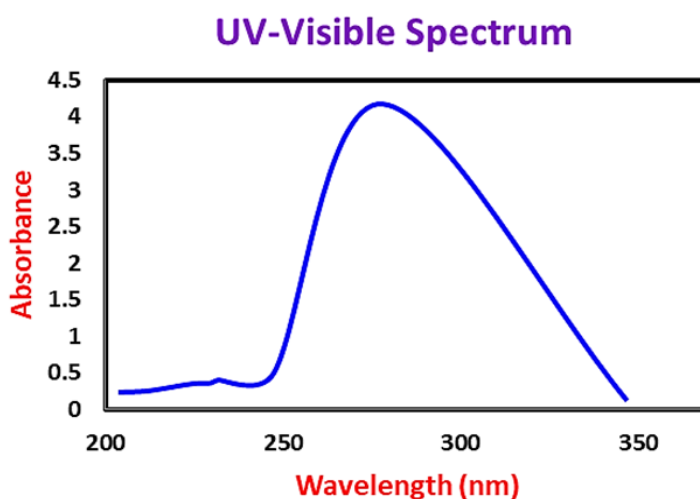


Fig.1: UV-Visible spectrum

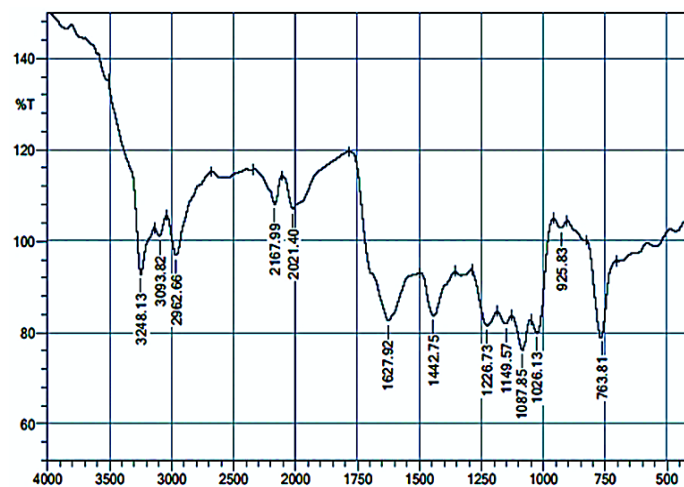


Fig.2: FT-IR spectrum

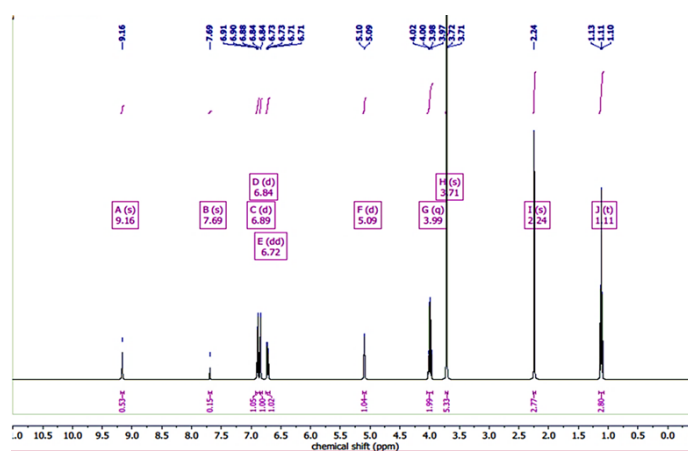


Fig.3: ¹H NMR spectrum

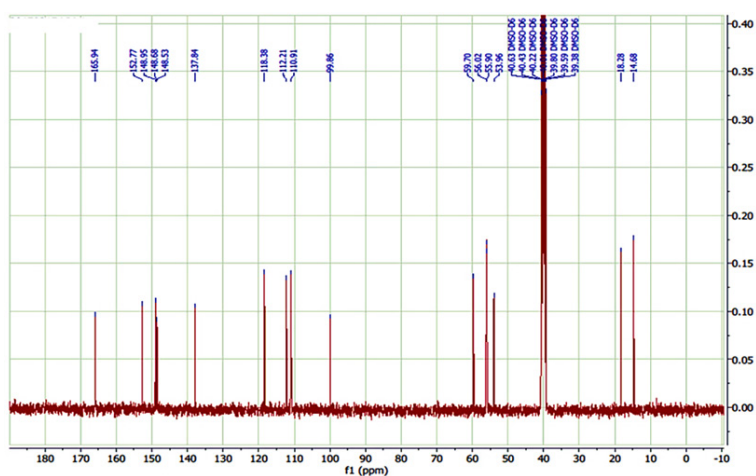


Fig.4: ¹³C NMR spectrum

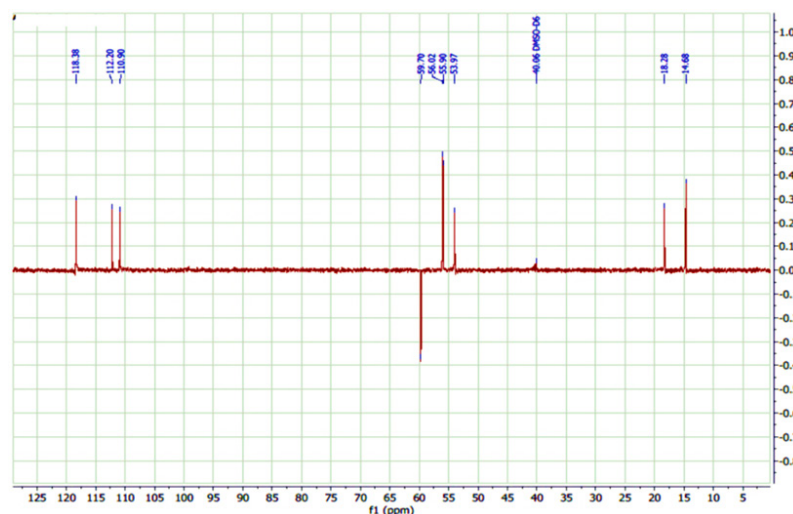


Fig.5: DEPT Spectrum

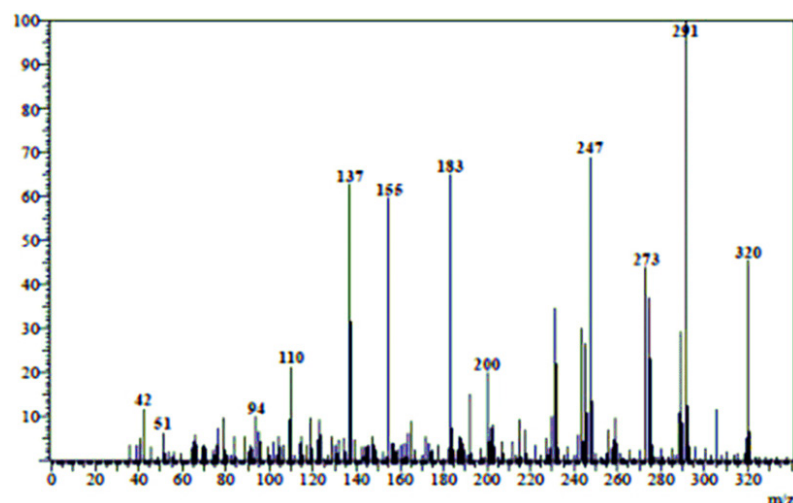


Fig.6: MASS Spectrum

Computational Study

Molecular Structure, Bond Lengths and Bond Angle Analysis

The optimized molecular structure of the title molecule is depicted in Figure 7. Molecular structures A, B, and C (Figure 8) represent presentation along various axes. The optimized molecular geometry provides a good deal of information about the spatial orientation of various atoms in a molecule. From optimized molecular structures, it can be easily seen that the EDTM molecule possesses C₁ point group symmetry due to the overall asymmetry of the molecule. Hence, the EDTM molecule is an

asymmetric top molecule. This data is a lot of helpful for the determination of various spectroscopic parameters. The geometrical parameters like bond lengths and bond angles for the title molecule have been set up by the DFT/B3LYP strategy with the 6-311++G (d,p) as premise set and are introduced in Table 2. The EDTM molecule comprises of two six-membered rings. The DFT computation predicts the benzene ring is planar (as expected) while the other ring is non-planar. The self-consistent field (SCF) energy of the title molecule at the DFT/B3LYP method with the 6-311++G (d,p) as basis set is found to be -1107.69 a.u. with dipole moment 4.05

Debye. The C10-C12, C13-O27, and C11-O29 bonds are 1.3603, 1.2174, and 1.219 Å long respectively. The bond angles of H21-C20-O28, C2-C1-C6, C1-O38-C39, and H21-C20-O28 are 112.8923

108.6969, 119.8669, 114.9448, and 108.6969° respectively. The bond angle and bond length data are in good agreement with the structure of the title molecule.

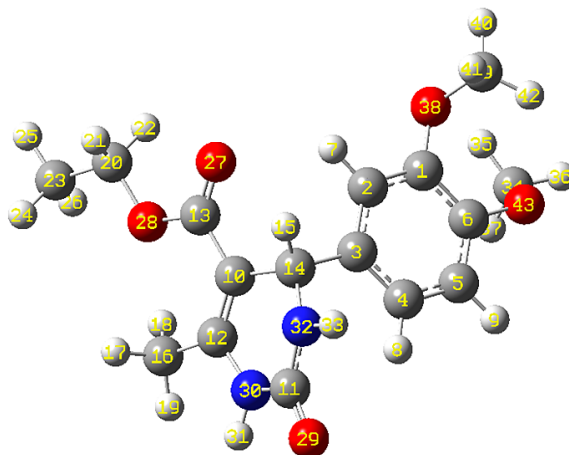


Fig.7: Optimized molecular structure

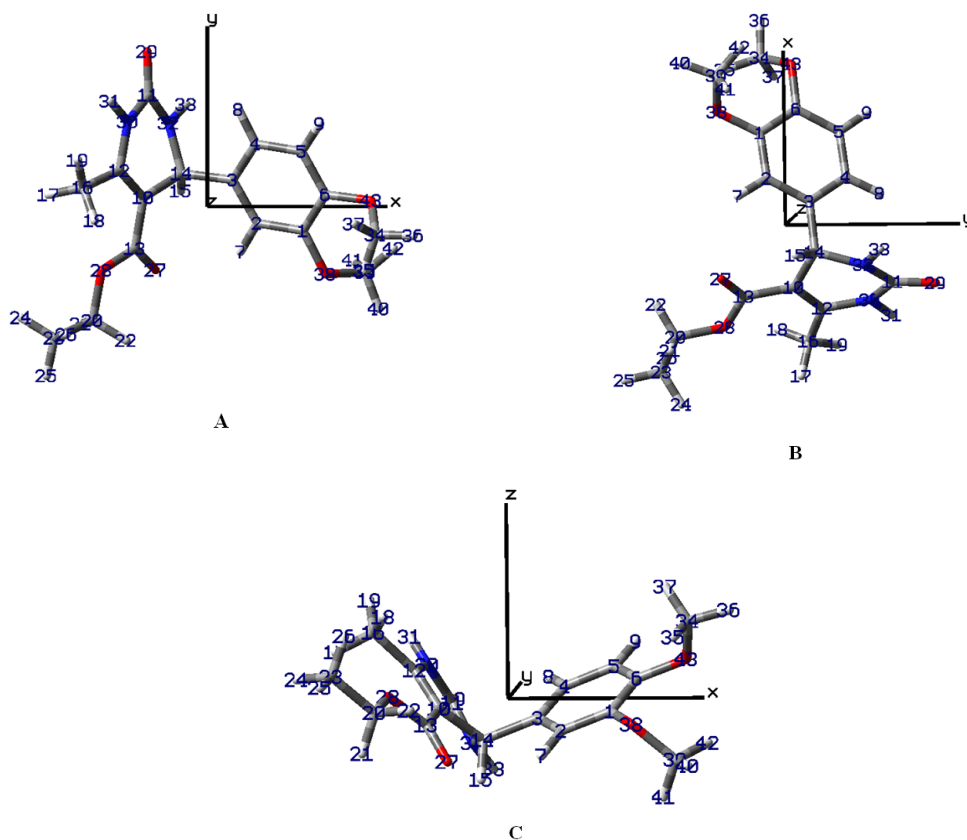


Fig.8: Optimized molecular structures along various axes

Table 2: Optimized geometrical parameters of IPPC by DFT/ B3LYP with 6-311++G (d,p) basis set

Bond lengths (Å)					
C1-C2	1.3921	C11-O29	1.219	C20-C28	1.449
C1-C6	1.4048	C11-N30	1.402	C23-H24	1.0926
C1-O38	1.3772	C11-N32	1.3595	C23-H25	1.0933
C2-C3	1.3989	C12-C16	1.5065	C23-H26	1.0925
C2-H7	1.0835	C12-N30	1.3855	N30-H31	1.0088
C3-C4	1.3977	C13-O27	1.2174	N32-H33	1.0098
C3- C14	1.5348	C13-O28	1.3562	C34-H35	1.0927
C4- C5	1.3931	C14-H15	1.0905	C34-H36	1.0897
C4-H8	1.0831	C14-N32	1.4658	C34-H37	1.0954
C5- C6	1.392	C16-H17	1.0918	C34-O43	1.4349
C5- H9	1.084	C16-H18	1.088	O38-C39	1.4345
C6-O43	1.3765	C16-H19	1.0922	C39-H40	1.0897
C10-C12	1.3603	C20-H21	1.0922	C39-H44	1.0953
C10-C13	1.4673	C20-H22	1.0921	C39-H42	1.0931
C10-C14	1.5275	C20-C23	1.5153	-	-
Bond angles (°)					
C2-C1-C6	119.8669	C10-C12-O30	118.535	C20- C23-H26	111.1729
C2-C1-H38	119.177	C16-C12-O30	113.8434	H24-C23-H25	108.1485
C6-C1-H38	120.9221	O10-C13-O27	123.2155	H24-C23-H26	108.553
C1-C2-C3	121.0938	C10-C13-C28	114.9106	H25-C23-H26	108.1352
C1-C2-H7	118.3975	C27-C13-H28	121.8701	C13-O28-C20	115.9493
C3-C2-H7	120.5047	C3-C14-N10	112.4642	C11-N30-N32	124.9462
C2-C3-C4	118.6253	C3-C14-H15	107.5333	C11-N30-H31	113.4226
C2-C3-C14	119.3121	C3-C4-N32	112.8923	C12-N30-H31	119.4272
C4-C3-C14	122.0623	H10-C14-N15	107.2569	C1-N32-C14	124.3583
C3-C4-C5	120.5362	C10-C14-H32	109.1721	C11-C12-H33	113.9896
C3-C4-H8	120.697	C15-C14-H32	107.22	C14-C12-H33	117.9436
C5-C4-H8	118.7648	C12-C16-H17	110.76	H35-C34-H36	109.9018
C4-C5-C6	120.7159	H12-C16-H18	111.2783	H35-C34-H37	109.7705
C4-C5-H9	120.91	H12-C16-H19	110.3105	H35-C34-O43	111.1473
C6-C5-C9	118.3736	H17-C16-H18	107.0429	H36-C34-H37	109.4042
C1-C6-C5	119.1268	H17-C16-H19	108.3867	H36-C34-O43	106.1786
C1-C6-C43	121.3621	H18-C16-H19	108.955	H37-C34-O43	110.3697
C5-C6-C43	119.4421	H21-C20-H22	107.6967	C1-O38-C39	114.9448
C12-C10-C13	126.0771	H21-C20-C23	112.0153	O38-C39-H40	106.2103
C12-C10-C14	119.3414	H21-C20-O28	108.6969	O38-C39-H41	110.4127
C13-C10-C14	114.5592	H22-C20-C23	112.0176	O38-C39-H42	111.1475
O29-C11-N30	121.0033	H22-C20-O28	108.6549	H40-C39-H41	109.3716
O29-C11-N32	125.3516	C23-C20-O28	107.6712	H40-C39-H42	109.868
N30-C11-N32	113.622	C20-C23-H24	111.189	H41-C39-H42	109.7619
C10-C12-C16	127.619	C20-C23-H25	109.5421	C6-O43-C34	115.0593
C2-C1-C6	119.8669	C10-C12-O30	118.535	C20- C23-H26	111.1729
C2-C1-H38	119.177	C16-C12-O30	113.8434	H24-C23-H25	108.1485

Mulliken Atomic Charges and Molecular Electrostatic Potential Surface Analysis

The Mulliken nuclear charges rely upon the electron density. The charge dispersion on the particles has a vital job in the field of quantum mechanical figurines for the molecular frameworks. The pictorial outline of the Mulliken nuclear charges of the EDMT molecule determined by the DFT/B3LYP strategy with a 6-311++G (d,p) premise set and given in Figure 6 and tabulated in Table 3. Mulliken atomic charges reveal that all the hydrogen atoms have a net positive

charge but H31 and H33 hydrogen atoms are highly electropositive with atomic charges of 0.240519 and 0.241399 respectively. This can be ascribed to attachment with a nitrogen atom in both cases. The C11 atom has the highest net positive charge (0.466199) whereas C23 atom has the highest net negative charge (-0.306972) amongst all carbon atoms. Out of the five oxygen atoms, O43 is having more negative charge density of -0.440306 and out of the two nitrogen atoms; N30 is more negative with -0.448179 Mulliken atomic charges.

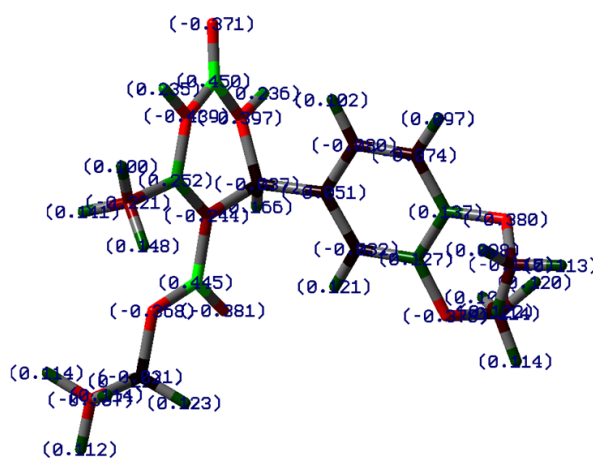


Fig.9: Mulliken atomic charges

Table 3: Mulliken atomic charges

Atom	Charge	Atom	Charge
1 C	0.104836	23 C	-0.306972
2 C	-0.003294	24 H	0.114512
3 C	-0.048593	25 H	0.113475
4 C	-0.053075	26 H	0.115685
5 C	-0.068050	27 O	-0.392430
6 C	0.152106	28 O	-0.400190
7 H	0.115950	29 O	-0.389454
8 H	0.100993	30 N	-0.448179
9 H	0.106250	31 H	0.240519
10 C	-0.257333	32 N	-0.404490
11 C	0.466199	33 H	0.241399
12 C	0.243106	34 C	-0.104141
13 C	0.455108	35 H	0.115058
14 C	-0.018689	36 H	0.122601
15 H	0.162141	37 H	0.103815
16 C	-0.209945	38 O	-0.380128

17 H	0.145091	39 C	-0.104903
18 H	0.148843	40 H	0.115880
19 H	0.097582	41 H	0.104293
20 C	-0.008970	42 H	0.101747
21 H	0.124053	43 O	-0.440306
22 H	0.127901	-	-

The molecular electrostatic surface potential (MESP) is the three-dimensional portrayal of the charge appropriations on molecules. The MESP diagram plotted by utilizing a 6-311++G (d,p) basis set is represented in Figure 10A and contour plot in Figure 10B. Over the span of on-going years, the MESP has risen as a convincing manual for investigating the molecular interactions. The phenomena like solvent effects, nucleophilic and electrophilic sites, hydrogen bonding forces, etc. could be predicted by the utilization of MESP plots. The different regions

of the MESP plot are represented by different colors. The red and yellow surfaces are the regions of large electron density and therefore linked with nucleophilic sites. Similarly, the blue colors indicate low electron density and associated with electrophilic sites. On the other hand, green surfaces suggest regions of zero potential. The MESP proposes, in the EDMT molecule, the benzene ring is highly reactive towards electrophiles. The positive potential is around hydrogen atoms.

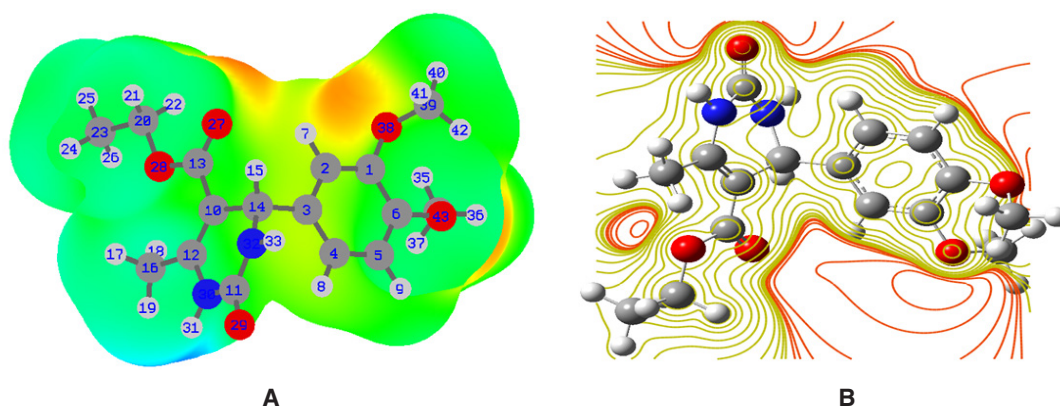


Fig.10: A Molecular electrostatic surface potential plot B Contour plot

Frontier Molecular Orbital and UV-Visible Spectral Analysis

The FMOs, highest occupied molecular orbital (HOMO) and lowest unoccupied molecular orbital (LUMO) are extremely crucial to anticipate the reactivity of the molecules. HOMO is the orbital which decides the nucleophilic ability whereas LUMO decides the electrophilic ability of the molecules. The energy gap between these two orbitals helps in deciding the stability. A smaller energy gap indicates high stability. Hence, one can foresee the chemical reactivity of the molecule. The expansion of the HOMO-LUMO energy gap prompts a reduction in adaptability, polarizability, and electron movement

in a molecule. The HOMO energy corresponds to ionization enthalpy (I) and LUMO energy to an electron affinity (A). The pictorial outline of the FMOs has been given in Figure 11. The assessment of the FMOs confirms that the electron excitation relates to the transition from the ground state to the first excited state and is essentially depicted by the one-electron move from HOMO to LUMO. In the EDMT molecule, HOMO is seen to be chiefly distributed over the benzene ring and the LUMO is distributed over the enone system. The energy gap between HOMO and LUMO suggests the inevitable charge transfer phenomenon is taking place within the EDMT molecule.

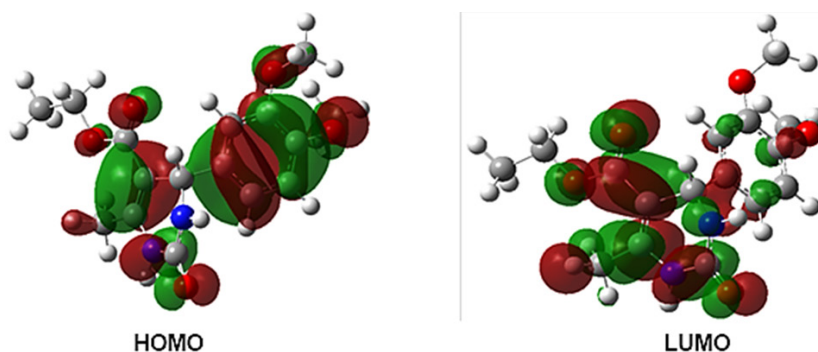


Fig.11: HOMO-LUMO pictures

Table 3: Electronic parameters

E_{Total} (a.u.)	E_{HOMO} (eV)	E_{LUMO} (eV)	ΔE (eV)	I (eV)	A (eV)
-1107.69	-6.39	-1.45	4.94	6.39	1.45

Note: Abbreviations: I, ionization potential; A, electron affinity; Note: $I = -E_{HOMO}$ & $A = -E_{LUMO}$

Table 4: Global reactivity parameters

χ (eV)	η (eV)	σ (eV ⁻¹)	ω (eV)	Pi (eV)	ΔN_{max} (eV)	Dipole moment (Debye)
3.92	2.47	0.40	3.11	-3.92	1.59	4.05

Note: $\chi = (I + A)/2$; $\eta = (I - A)/2$; $\sigma = 1/\eta$; $\omega = \text{Pi}/2\eta$; $\text{Pi} = -\chi$; $\Delta N_{max} = -\text{Pi}/\eta$.

Abbreviations: χ , electronegativity; η , absolute hardness; σ , global softness; ω , global electrophilicity; Pi, chemical potential; ΔN_{max} , maximum no. of electron transferred.

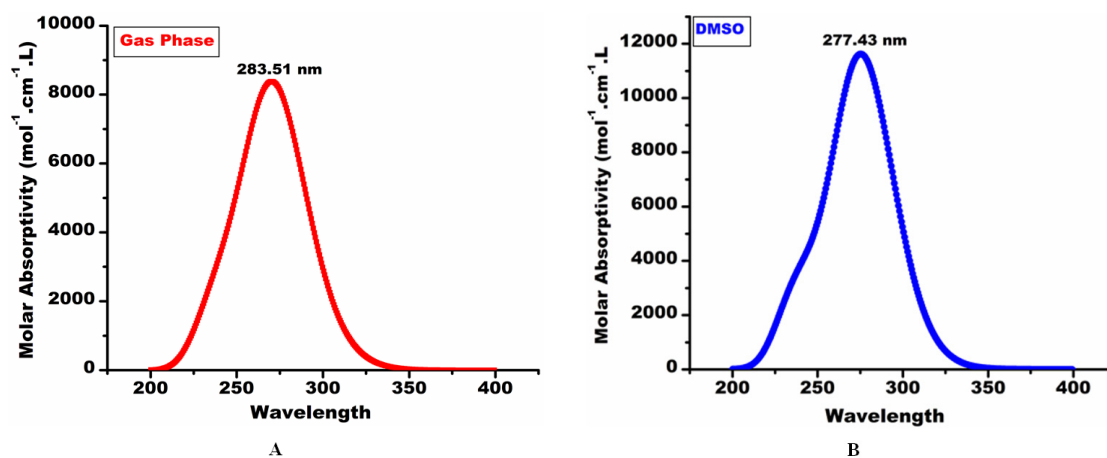


Fig.12: A Theoretical UV-Visible spectrum in gas phase B Theoretical UV-Visible spectrum in DMSO solvent

Table 4: Absorption energies (λ in nm), Oscillator strength (f), and transitions of EDTM computed at TD-B3LYP/6-311G++ (d,p) level of theory for B3LYP/6-311G ++ (d,p) optimized geometry in gas phase

Sr. No.	Absorption Wavelength (nm)	Excitation energy (eV)	Excited state	Electronic Transition	Oscillator strength (f)
1	283.51	4.3732	1	85 -> 86	0.62706
2	269.94	4.5930	2	84 -> 86	0.62706
3	261.36	4.5930	3	83 -> 86	0.66620
4	245.66	5.0470	4	83 -> 87	0.10131

Table 5: Absorption energies (λ in nm), Oscillator strength (f), and transitions of EDTM computed at TD-B3LYP/6-311G++ (d,p) level of theory for B3LYP/6-311G ++ (d,p) optimized geometry in DMSO solvent

Sr. No.	Absorption Wavelength (nm)	Excitation energy (eV)	Excited state	Electronic Transition	Oscillator strength (f)
1	277.43	4.4691	1	85 -> 86	0.68511
2	273.97	4.5255	2	84 -> 86	0.67699
3	254.77	4.8665	3	83 -> 86	0.62180
4	244.66	5.0675	4	83 -> 87	0.24938

The different electronic parameters of the EDTM molecule are organized in Table 3 and reactivity descriptors in Table 4. In light of HOMO and LUMO energies and by utilizing Koopmans' hypothesis different global reactivity descriptors like electronegativity (χ) absolute hardness (η) global softness (σ) global electrophilicity (ω) chemical potential (P_i), the maximum number of electron transferred (ΔN_{max}) are calculated. The title molecule EDTM is a good electrophile ($\omega = 3.11$ eV). The ΔN_{max} estimation of the EDTM molecule is 1.59 eV indicating charge transfer. The energy gap is 4.94 eV which indicates an inevitable electron movement within the title molecule. Crucially, the theoretical UV-Visible spectrum of the EDTM is correlated with the experimental UV-Visible spectrum to aid the computed results. The theoretical UV-Visible absorption peaks are 283.51 nm in the gas phase and 277.43 nm (Figure 12A) in the DMSO solvent (Figure 12B). The experimental UV-Visible absorption peak is 278.00 nm in the DMSO solvent. The great agreement between the theoretical and experimental UV-Visible absorption values supports

the computed results. Absorption energies (λ in nm), excitation energies, electronic transitions, and oscillator strength (f) of EDTM are computed at TD-B3LYP/6-311++G (d,p) level of theory for B3LYP/6-311++G (d,p) optimized geometry in the gas phase and DMSO solvent. The absorption band is slightly shifted to a lower wavelength from the gas phase to the DMSO solvent. At the point when the ground state is more polar than the excited state, the polar solvents settle the ground state more than the excited state. So in general there is an expansion in the energy gap between the ground state and excited state bringing about the blue shift.

Thermodynamic Parameter Analysis

Considering the vibrational assessment, the distinctive thermodynamic properties were presented from the computed vibrational frequencies and are recorded in Table 6. All the thermodynamic data revealed in this would be valuable for additional assessment and could be used to infer other thermodynamic boundaries as demonstrated by connections of thermodynamic capacities.

Table 6: Thermochemical information of EDMT

Parameter	Value
E total (kcal mol ⁻¹)	228.433
Translational	0.889
Rotational	0.889
Vibrational	226.656
Heat Capacity at, constant volume	78.060
Cv (cal mol ⁻¹ K ⁻¹)	2.981
Translational	2.981
Rotational	72.098
Vibrational	
Total entropy S (cal mol ⁻¹ K ⁻¹)	144.603
Translational	43.186
Rotational	35.147
Vibrational	66.270
Zero point Vibrational Energy Ev ₀ (Kcal mol ⁻¹)	216.07087
Rotational constants (GHZ)	0.30045
	0.16655
	0.13128

Conclusions

In outline, the EDMT molecule is synthesized by a three-component reaction. The structure of the EDMT molecule is affirmed based on the basis of UV-Visible, FT-IR, ¹H NMR, ¹³C NMR, and Mass spectral methods. The geometry of the title molecule was optimized by using a 6-311++G (d,p) basis set, and the geometrical parameters like bond lengths and bond angles were computed at the same level of theory. The title molecule is an asymmetric top molecule with C₁ point group symmetry. The FMO study is discussed and various chemical, electronic, and quantum chemical parameters are studied to analyze the chemical reactivity of the title molecule. The HOMO-LUMO energy gap suggests that the charge transfer phenomenon is taking place within the molecule. The theoretical wavelength in the gas phase is higher than in the DMSO solvent. The theoretical UV-Visible spectrum is correlated with the experimental UV-Visible spectrum and a very nice agreement is found. The MESP plot reveals that electrophiles would attack at the benzene ring.

The thermodynamic properties like total energy, total molar heat capacity, total entropy, zero-point vibrational energy, and rotational constants have been figured and discussed.

Acknowledgments

Authors acknowledge central instrumentation facility (CIF), Savitribai Phule Pune University, Pune for NMR, MGV's Pharmacy College, Nashik for UV-Visible, and central instrumentation centre (CIC), KTHM College, Nashik for FT-IR spectral analysis. Authors also would like to thank Lokenete Vyankatrao Hiray Arts, Science and Commerce College Panchavati, Nashik and Arts, Science and Commerce College, Manmad for permission and providing necessary research facilities. Authors would like to express their sincere and humble gratitude to Prof. (Dr.) Arun B. Sawant for Gaussian study. Dr. Aapoorva P. Hiray, Coordinator, MG Vidyamandir institute, is gratefully acknowledged for the Gaussian package.

Funding

We have not received any kind of fund for the research work.

Conflict of Interest

Authors declared that he do not have any conflict of interest regarding this research article.

References

1. de Fatima, A., Braga, T.C., Neto, L.D.S., Terra, B.S., Oliveira, B.G., da Silva, D.L. and Modolo, L.V., 2015. A mini-review on Biginelli adducts with notable pharmacological properties. *Journal of advanced research*, 6(3), pp.363-373.
2. Matos, L.H.S., Masson, F.T., Simeoni, L.A. and Homem-de-Mello, M., 2018. Biological activity of dihydropyrimidinone (DHPM) derivatives: A systematic review. *European journal of medicinal chemistry*, 143, pp.1779-1789.
3. Kaur, R., Chaudhary, S., Kumar, K., Gupta, M.K. and Rawal, R.K., 2017. Recent synthetic and medicinal perspectives of dihydropyrimidinones: A review. *European journal of medicinal chemistry*, 132, pp.108-134.
4. Mostafa, A.S. and Selim, K.B., 2018. Synthesis and anticancer activity of new dihydropyrimidinone derivatives. *European journal of medicinal chemistry*, 156, pp.304-315.
5. Singh, K., Singh, K., Wan, B., Franzblau, S., Chibale, K. and Balzarini, J., 2011. Facile transformation of Biginelli pyrimidin-2 (1H)-ones to pyrimidines. In vitro evaluation as inhibitors of Mycobacterium tuberculosis and modulators of cytostatic activity. *European journal of medicinal chemistry*, 46(6), pp.2290-2294.
6. October, N., Watermeyer, N.D., Yardley, V., Egan, T.J., Ncoakazi, K. and Chibale, K., 2008. Reversed Chloroquines Based on the 3, 4-Dihydropyrimidin-2 (1H)-one Scaffold: Synthesis and Evaluation for Antimalarial, β -Haematin Inhibition, and Cytotoxic Activity. *ChemMedChem: Chemistry Enabling Drug Discovery*, 3(11), pp.1649-1653.
7. Kumarasamy, D., Roy, B.G., Rocha-Pereira, J., Neyts, J., Nanjappan, S., Maity, S., Mookerjee, M. and Naesens, L., 2017. Synthesis and in vitro antiviral evaluation of 4-substituted 3, 4-dihydropyrimidinones. *Bioorganic & medicinal chemistry letters*, 27(2), pp.139-142.
8. Ajitha, M., Rajnarayana, K. and Sarangapani, M., 2011. Synthesis and evaluation of new 3-substituted-[3, 4-dihydropyrimidinones]-indolin-2-ones for analgesic activity. *International Res J Pharm*, 2(7), pp.80-84.
9. Attri, P., Bhatia, R., Gaur, J., Arora, B., Gupta, A., Kumar, N. and Choi, E.H., 2017. Triethylammonium acetate ionic liquid assisted one-pot synthesis of dihydropyrimidinones and evaluation of their antioxidant and antibacterial activities. *Arabian Journal of chemistry*, 10(2), pp.206-214.
10. Tale, R.H., Rodge, A.H., Hatnapure, G.D. and Keche, A.P., 2011. The novel 3, 4-dihydropyrimidin-2 (1H)-one urea derivatives of N-aryl urea: synthesis, anti-inflammatory, antibacterial and antifungal activity evaluation. *Bioorganic & medicinal chemistry letters*, 21(15), pp.4648-4651.
11. Singh, O.M., Singh, S.J., Devi, M.B., Devi, L.N., Singh, N.I. and Lee, S.G., 2008. Synthesis and in vitro evaluation of the antifungal activities of dihydropyrimidinones. *Bioorganic & medicinal chemistry letters*, 18(24), pp.6462-6467.
12. Dhumaskar, K.L., Meena, S.N., Ghadi, S.C. and Tilve, S.G., 2014. Graphite catalyzed solvent free synthesis of dihydropyrimidin-2 (1H)-ones/thiones and their antidiabetic activity. *Bioorganic & medicinal chemistry letters*, 24(13), pp.2897-2899.
13. Russowsky, D., Canto, R.F., Sanches, S.A.,